Physica A 405 (2014) 92–103

Contents lists available at ScienceDirect

Physica A

journal homepage: www.elsevier.com/locate/physa

Collective behavior and the identification of phases in bicycle pelotons

Hugh Trenchard [a,*], Ashlin Richardson [b], Erick Ratamero [c], Matjaž Perc [d]

[a] 805 647 Michigan Street, Victoria BC, Canada V8V 1S9

[b] University of Victoria, Department of Computer Science, PO Box 1700, Victoria BC, Canada V8W 2Y2

[c] University of Warwick, MOAC DTC - Senate House, Gibbet Hill Road CV4 7AL Coventry, UK

[d] Faculty of Natural Sciences and Mathematics, University of Maribor, Koroška cesta 160, SI-2000 Maribor, Slovenia

HIGHLIGHTS

- A method for identifying phases in bicycle pelotons is proposed.
- Collective behavior in bicycle pelotons is characterized by two distinct phases.
- Lateral synchronization occurs only in the high density phase.
- High velocities give rise to the low density "stretched" phase.
- Collective behavior reflects both energy savings and tactics in competition.

ARTICLE INFO

Article history:
Received 17 February 2014
Available online 12 March 2014

Keywords:
Collective behavior
Flocking
Phase transition
Peloton
Cycling

ABSTRACT

As an aggregate of cyclists, a peloton exhibits collective behavior similar to flocking birds or schooling fish. Positional analysis of cyclists in mass-start velodrome races allows quantitative descriptions of peloton phases based on observational data. Data from two track races are analyzed. Peloton density correlates well with cyclists' collective power output in two clear phases, one of low density, and one of high density. The low density "stretched" phase generally indicates low frequency positional-change and single-file synchronization. The high density "compact" phase may be further divided into two phases, one of which is a laterally synchronized phase, and another is a high frequency and magnitude positional-change phase. Phases may be sub-divided further into acceleration and deceleration regimes, but these are not quantified here. A basic model of peloton division and its implications for general flocking behavior are discussed.

1. Introduction

A peloton may be defined as a group of cyclists that are coupled together through the mutual energy benefits of drafting, whereby cyclists follow others in zones of reduced air resistance. Although the interactions among individual cyclists are in principle very simple – each cyclist takes a turn leading and then returns to the pack – the collective behavior of the peloton is very complex. This is characteristic for social interactions in general. These interactions usually involve only a few individuals at a time, yet may give rise to non-trivial global phenomena, like opinion formation, cultural dissemination, evolution of cooperation, and the emergence of hierarchy in initially egalitarian societies [1–4].

* Corresponding author.
E-mail addresses: htrenchard@shaw.ca (H. Trenchard), ashy@uvic.ca (A. Richardson), e.martins-ratamero@warwick.ac.uk (E. Ratamero), matjaz.perc@uni-mb.si (M. Perc).

http://dx.doi.org/10.1016/j.physa.2014.03.002
0378-4371/

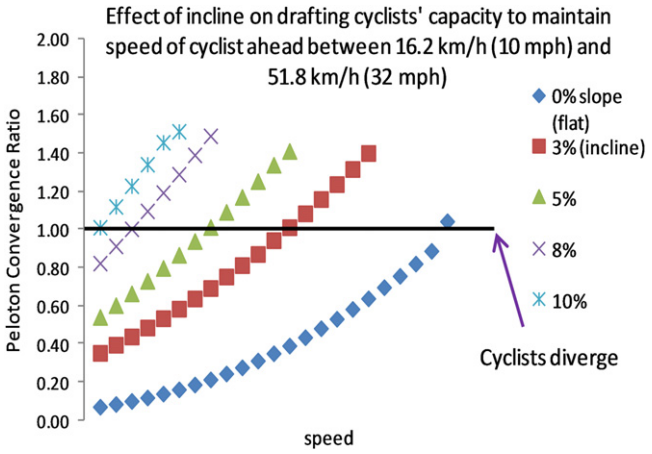

Fig. 1. Illustration of the application of the peloton convergence ratio (PCR), demonstrating the effect of increasing slope on a drafting cyclist's capacity to maintain the speed of a front cyclist. Using an approximate energy savings of 1% per 1.6 km/h (1% per miles/h) starting at 16.2 km/h (10 miles/h) to a maximum of 51.8 km/h (32 miles/h), each point represents 1.6 km/h (1 mile/h), also corresponding to 1% energy savings by drafting below PCR = 1.00. *Source:* Figure adapted from Ref. [11].

Investigations of conceptually similar complex systems have a long tradition in condensed matter physics. Among the most important features of complex systems is the emergence of phase transitions [5], which can be traced back to the Ising model [6]. In fact, the comprehensive understanding of the collective behavior of systems at phase transition points can be considered as a major intellectual revolution of statistical physics during the past century. Strong interactions between particles result in increasing correlation lengths, which render microscopic details of the system irrelevant from the viewpoint of its macroscopic behavior. As a result, universality classes have been established in which seemingly very different systems behave identically.

The parallelism between interactions between particles and spins and the interactions among living organisms is the motivation behind many applications of statistical physics methods and models to describe large-scale complex social and natural phenomena. The applications range from fractal growth [7,8] to correlations in economy [9] and animals on the move [10]. Here we wish to extend the scope of this theory to the collective behavior in bicycle pelotons, which to the avid cyclists among the readers will be familiar as the stage for intriguing tactical and positional competition.

1.1. Coupling model for cyclists in peloton

Peloton dynamics have been characterized by four major phases, and oscillations among phases were modeled as occurring within threshold ranges of a parameter called the "peloton convergence ratio" ("PCR") [11]. The Peloton Convergence Ratio describes the coupled power-output relationship between two cyclists, one being in a non-drafting position, and the other being in a drafting position. The Peloton Convergence Ratio quantifies the power reduction benefits of drafting at a given speed.

$$\mathrm{PCR} = \frac{\left[P_{\mathrm{qfront}} - \left(P_{\mathrm{qfront}} * \left(\frac{D}{100}\right)\right)\right]}{P_{\mathrm{MSO}}}. \tag{1}$$

In (1) P_{qfront} is the power output of the front rider at the given speed (the same power output that would be required by the drafting (following) rider to maintain the speed set by the front rider, *were the following rider not drafting*—hence "required output"); D is the percentage of energy saved by drafting; P_{MSO} is the maximal sustainable output (MSO) of the drafting cyclist, subsequently defined in more detail.

PCR is more simply described as a ratio of the following rider's required output for the given speed, minus drafting benefit D, over her maximum output, where the speed and drafting component are determined by the front rider. Differences in equipment, body frontal surface area or body position, are ignored.

The required output, as set by the non-drafting front rider, may exceed the maximal sustainable output of the following rider. However, the *actual* output of the following rider at the speed set by the front rider is that which has been reduced by drafting benefit D. When PCR < 1, the following rider's actual output is less than her maximal sustainable output, and she maintains the speed set by the front rider. When PCR > 1, the required output exceeds the drafting rider's actual output and her maximal sustainable output, and the two riders will de-couple, as shown in Fig. 1.

For example, a drafting (following) cyclist with a hypothetical maximum sustainable output of 349 W (based on the range of power outputs reported by Ref. [12]) on a flat, windless, course can maintain the speed of a rider ahead (who may or may not also be drafting behind other riders) up to about 32 miles/h (51.8 km/h), above which a stronger rider will ride away from the weaker cyclist, when PCR > 1. On a 3% grade, the same drafting cyclist will be able to maintain the speed of a rider ahead up to about 22 miles/h (35.4 km/h), above which a stronger front rider will pull ahead. At grades of 10% or more

the drafting benefit is negligible due to low speeds, and a cyclist in front who is even marginally stronger than the drafting cyclist, will pull ahead.

PCR may be calculated as a collective value for all drafting riders coupled to the front rider; it is a global parameter that correlates with collective changes in phase. Peloton density and cyclists' positional change are similar collective parameters that correlate with change in phase. Here "positional-change" refers to the change in relative order of the cyclists from the front of the group in the direction of motion, to the back.

In summary, the following phases were earlier qualitatively identified [11]: (i) Relaxed (high density, low frequency positional-change): low PCR < 1. Cyclists proceed at comparatively low power outputs; (ii) Convective (high density, high frequency positional-change): intermediate PCR < 1. Riders advance up peloton peripheries, passing riders in central positions where density is high. Passing occurs in continuous rotation; (iii) Synchronized (low density, low frequency positional-change): high PCR < 1. As riders approach maximal sustainable output, PCR approaches 1, and cyclists' self-organize into single-file (one-behind-another), and (iv) Disintegrated (very low density, low frequency positional-change): Riders de-couple and separate. PCR > 1.

Confirmation of the convective phase has been shown by simulation [13]. Stop and go waves have been reported for cyclists in single-file [14]. Similarly, in Ref. [15] a speed–density model for bicycles, and mixed electric bicycle and bicycles was investigated. However, [14,15] do not consider the competitive dynamics of pelotons and their concomitant energetic demands and coupling due to drafting, and do not demonstrate mass-start peloton dynamics. As a result, there currently does not appear to be any independent empirical study demonstrating the dynamics of peloton phases. Here phase boundaries are indicated empirically as a function of cyclists' variation in position and Peloton Convergence Ratio, according to data collected from two mass-start velodrome races.

2. Methods

2.1. Data collection

Video data of mass-start track races during the British Columbia Provincial track championships (August 23–25, 2013) were obtained by using a Sony Handycam 60× optical zoom hand-held camera. The camera operator stood on an adjustable platform, positioned centrally at the in-field of the 333.3 m outdoor Westshore Velodrome, located in the municipality of Colwood, British Columbia. The platform was raised to approximately 15 ft above ground level to reduce visual obstruction from tents and other objects present on the track in-field. The operator rotated the camera ensuring to the extent possible that all riders were continuously in the camera field-of-view. Maximum platform height was not achieved due to safety considerations, and some minimal obstruction between the camera and track from in-field tents remained.

The data analyzed here were collected from two races: the women's 30 lap (10 km) points race (on the morning of August 24, 2013) and the women's 20 lap (6.66 km) scratch race (on the afternoon of August 25, 2013). Points races involve the accumulation of points by finishing order on designated laps. For the specific points race recorded, points were assigned to the top four riders every 6th lap. Lapped riders receive negative value points. The winner is the rider with the greatest number of points accumulated. Scratch race finishing order is determined by the order on the final lap only.

The women's points race involved 14 competitors distributed by age as follows: 5 senior ($>$19 yr), 4 (17–19 yr), 4 (15–17 yr), and 1 (13–15 yr). The women's scratch race involved the same group of competitors (excepting two from the 15–17 yr category) for a total of 12 competitors.

Race speeds were calculated on the basis of two timing points, one positioned approximately one-third around the track at 133.3 m (the location of a 200 m remaining line on the track), and the other positioned at the start/finish line at 333.3 m. The speed data are of comparatively coarse granularity as a result; while resolution for correlation between PCR and positional dynamics is not optimal, data and results are sufficient for useful analysis.

Among the various mass-start events held the weekend of the B.C. Championships (individually timed events were not considered for this study) the women's points and scratch races were selected for analysis for the reasons as follows. First, the numbers of competitors in these races were highest among all the mass-start events that weekend. In view of the hypothesis that larger pelotons, to some threshold number not reached in these cases, will provide more accurate data for the study of peloton collective motion, the data from these races were the best available. Secondly, the pelotons in these two races were sufficiently cohesive such that the groups generally stayed within the camera field-of-view for the majority of the duration of each race. By comparison, other mass-start races recorded that weekend had less cohesive groups, making it impossible to track all riders with a single camera. Thus, among the mass-start events recorded during the two days of racing events, those analyzed here yielded the most suitable data for the study of peloton dynamics.

Compared to road races or other kinds of mass-start bicycle races, such as mountain bike or cyclo-cross races, mass-start track races represent highly controlled conditions for the study of peloton dynamics. In mountain-bike and cyclo-cross races the courses are generally single-track, i.e., obstacles may force cyclists to ride single-file with limited passing opportunities. For such races it is not possible to observe the full scope of peloton dynamics. Pelotons larger than those studied here (e.g. those observed in road races, which may include 50 riders or more) would provide useful data for the understanding of peloton dynamics. However for road races the topography, width, and circuitousness of the course are entirely variable, making data acquisition difficult. As a result of their uniform topography, track races permit convenient data collection,

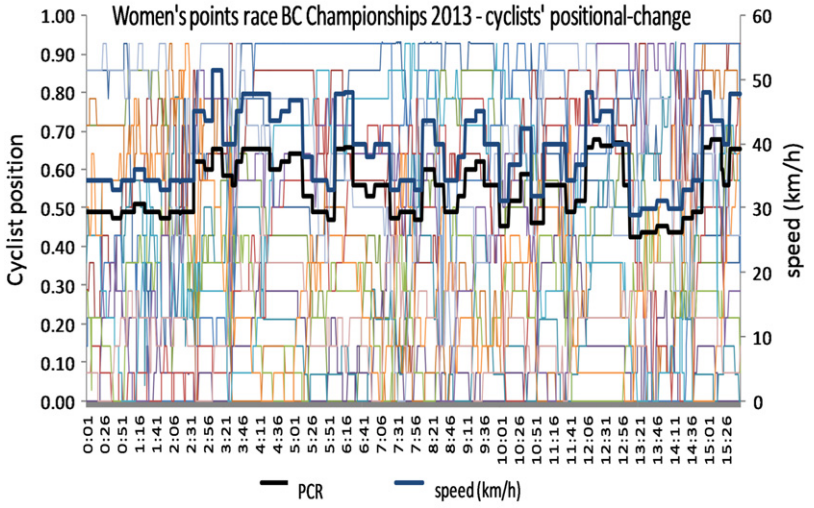

Fig. 2. Women's 30-lap points race, competitors' positional-change from start to finish. Heavy blue curve is speed; heavy black curve is Peloton Convergence Ratio (PCR).

which may be obtained from a central in-field location. Distances and speeds are also easily measured. Moreover, the bowl-shape of the velodrome reduces wind effects.

2.2. Determining cyclists' relative positions

The video data were analyzed visually for the entire duration of both races to determine the cyclists' relative positions. Position data were obtained by uniquely identifying the cyclists and recording the change in relative ordering among them. From the moment of crossing the start line at the commencement, data points were derived second-to-second for each cyclist (2):

$$P = (C_{\text{ahead}}/C_{\text{total}})/\Delta t. \tag{2}$$

Here P is position; C_{ahead} is the number of riders ahead, discounting those cyclists aligned laterally (those directly beside or behind up to approximately half a bicycle-length); C_{total} is the total number in the group; Δt is the period between observations, in seconds. Here positional data were generated via (2) by counting (for each cyclist) the number of cyclists ahead, dividing that result by the total number of riders in the group (14 in the points race, and 12 in the scratch race). Measurements were made on a second-to-second basis ($\Delta t = 1$ s).

In Ref. [16] a positional-change method was used to study the dynamics of sheep flocks. This involved observing the changes in displacements of individual sheep, relative to the centroid of the flock. Other positional-change analysis methods have been used to study flocking dynamics, e.g., those involving changes in domains of danger relative to predation risk [17, 18], however it appears the positional-change method indicated by (2) is novel in the context of flocking dynamics.

Broadly applicable, (2) yields a positional ratio that may be used to draw comparisons between different flocking systems (independent of the flock sizes). A drawback is that relative lateral positions are not accounted for. Nonetheless, while precise relative lateral positions are not indicated by this method, periods of lateral alignment are revealed in the positional-change curves, as shown in Figs. 2–5. A further limitation of (2) is that, outside of the peloton context, flocking behavior rarely occurs in mean straight-line trajectories for sufficiently long periods to obtain data accurately representative of such positional-changes. In such cases, however, a correction for mean trajectory may allow (2) to be applied to the dynamics of more general flocking situations, particularly those in two-dimensions.

2.3. Drafting parameter

For the parameter drafting parameter D, a simplified speed-varying estimate of 1% per (miles/h) may be applied, which approximately tracks empirically obtained results in Ref. [19]. A more comprehensive estimate for the drafting parameter is given in Ref. [20]. In Ref. [20] an equation is derived based on analysis and data given in Ref. [21], and derives the drafting benefit as a ratio of cyclists' power requirements in drafting positions to power requirements in non-drafting positions. This value is 0.62 adjusted for by wheel spacing parameters which we do not apply here, since wheel spacing is continually changing, and difficult to measure from the video data. Further power output parameters were applied as set out in Ref. [22].

Aerodynamic drag due to changes in cyclist positions [23] and wheel spacing [20] are additional factors that should be considered in the estimation of D. Consequently the estimates for D used here are adequate for our purposes, although future studies should consider increasingly accurate and realistic estimates for D.

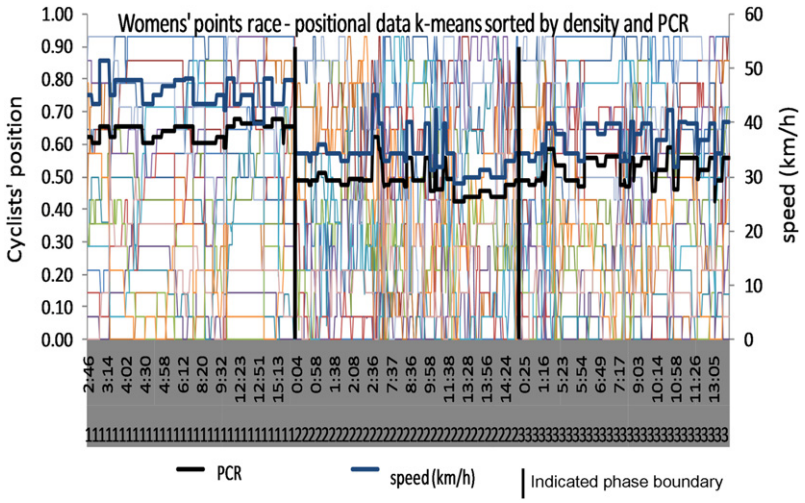

Fig. 3. Points race data sorted using *k*-means clustering of PCR and density. Vertical lines indicate cluster boundaries 1–3. Clusters are also shown in the row at graph bottom.

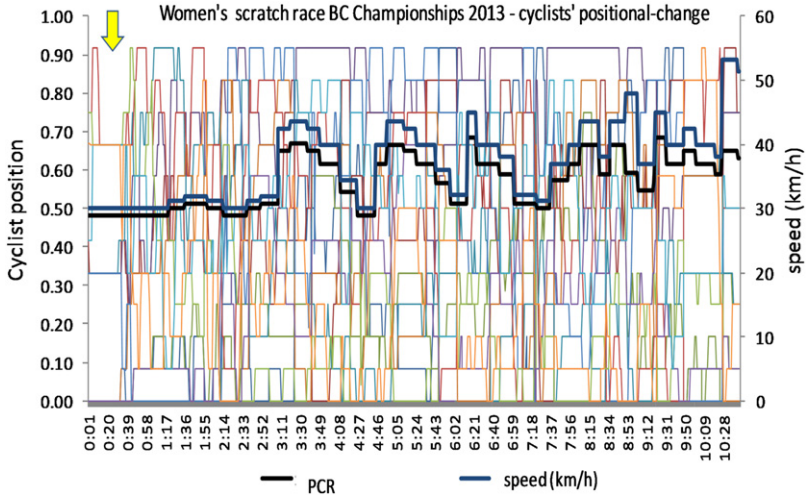

Fig. 4. Women's 20-lap scratch race: competitors' positional-change from start to finish. Yellow arrow indicates period of lateral (side-by-side) synchronized riding, where each of three main horizontal lines represents approximately 4 riders proceeding laterally across the track.

2.4. Maximal sustainable output (MSO)

Broadly speaking, an athlete's MSO is the maximum power output sustainable for a given period of time. Typically an athlete's absolute maximum output along with three domains of sub-maximal output, are considered [24]. The measurement of thresholds representative of such MSO domains varies in the literature [25]. For example, a sprint effort where the absolute maximum output is achieved has been defined as the period for which peak power output is attained within 5–10 s of all-out effort [24,26]; others describe sprints with duration of 15 s [27] or as long as 30 s [28]. Domains of sub-maximal physiological output have been described as moderate, heavy, and severe [24]. Boundaries for these are variously described involving lactate or gas exchange thresholds (boundary between moderate and heavy), or critical power (boundary between heavy and severe); the upper limit of severe is determined by the work rate that results in attainment of maximal oxygen uptake [24]. Alternative descriptions include fatigue or exhaustion thresholds according to metabolic, neuromuscular, or psychological indicators [29].

Also, fatigue alters MSO. Fatigue has been defined as a reversible, exercise-induced reduction in maximal power output, even though the task can be continued [30]. Because of frequent opportunity to recover while drafting, or during short-term periods not requiring pedaling (e.g., downhill) bicycle racing is especially conducive to alternations between short term periods of high output, with periods of recovery due to reversible fatigue. Cycling races therefore naturally involve collective MSO fluctuations. This may be generalized to all competitive events characterized by bursts of near-maximal efforts followed by recovery, as well as collective animal behaviors such as migration, resource scavenging, and escape from predators.

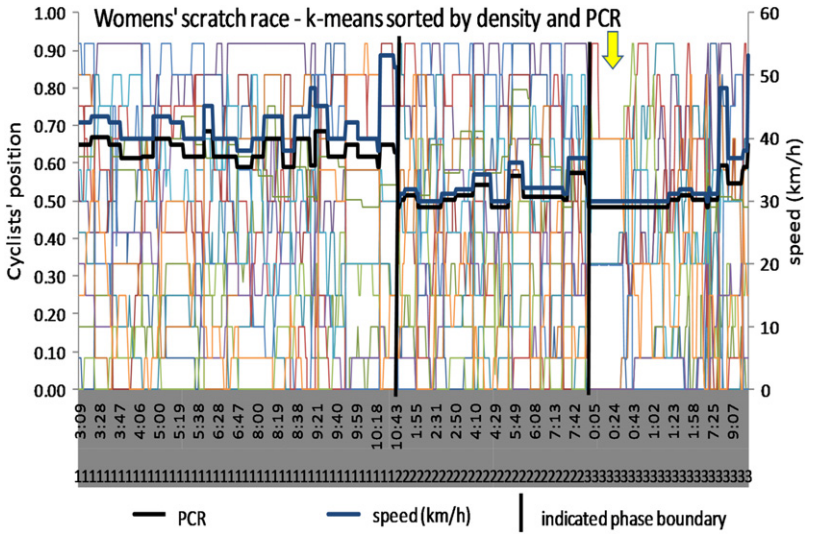

Fig. 5. Scratch race data sorted using *k*-means of density and PCR. Minimal distinction is observed in PCR and speed between clusters 2 and 3, although cluster 3 exhibits higher mean density (Table 3), and contains a period in which riders exhibit low-output lateral (side-by-side) synchronized riding, indicated by the yellow arrow. Visually, a similar phase appears to the left of the first vertical bar at the boundary between cluster 1 and cluster 2, although given its higher PCR and speed, it is grouped in phase 1. Arguably these regions of lateral synchronization comprise a separate phase.

Generally research regarding the power capacity drop experienced during recovery is limited. However, [31] reported a 28% power reduction between 10 and 20 s of a sprint relative to the first 10 s. A similar percentage capacity drop was reported in Refs. [32,33] during 10 s recovery periods following 5 s sprints, while much greater recovery was achieved after 30 s of rest. This indicates that recovery increases significantly between 10 and 30 s of recovery time, resulting in a lower than 28% average capacity drop over a 30 s recovery period. For our purposes, an estimated 28% capacity drop is applied and counted for 15 s following a sprint, with no consideration of a changing rate over that period and assuming that maximal recovery occurs after 15 s. In reality the cyclists may not have approached maximal recovery after 15 s, but the duration provides a reasonable value for this study.

While power capacity falls during recovery periods, successive maximal efforts, following recovery periods, also result in incremental reductions in power output capacity over succeeding efforts. Reductions in successive sprint outputs typically develop rapidly after the first sprint [33]. The study in Ref. [34] found that repeated 6 s sprints with 30 s recovery intervals result in reductions of maximal power capacity for succeeding sprint efforts at ∼94%, ∼92%, and ∼89% of the initial maximum effort measured.

For this study, accurate physiological data regarding individual maximal sustainable output profiles were not obtained. Consequently, for the purposes of this study, reasonable approximations demonstrate changing maximal sustainable outputs during the course of a race, and the effects upon PCR and phases of aggregate peloton dynamics. In addition to the limitation in accurate maximal sustainable output data in this study, speed data (being derived from only two timing points per lap) are also coarse-grained. Thus changes in peloton dynamics that correlate to changes in speed and PCR are demonstrated with relatively low resolution. However, if our objective is to show a relationship between changing Peloton Convergence Ratio and phases, then (1) must account for a dynamic maximal sustainable output.

Despite the absence of accurate MSO data, there is good correlation between power output and track race speeds. Since track topography does not vary, speed data may be used for a reasonable approximation of MSO instead of the power output parameter (the preferred indicator). While cyclists do ascend and descend on the banked curves, these changes occur over relatively short distances (in the range of several meters) so we make the reasonable assumption that, overall, deceleration experienced during ascent will offset the acceleration experienced during descent. Also, bicycle angles are maintained at approximately 90° relative to the track surface while cornering; approximately constant velocity is maintained around curves [35]. Moreover, despite some ambient wind that could possibly affect speeds on the windward straightaways, the wind shelter provided by the velodrome is quite favorable, so wind effects are ignored for the purposes of this study. For this study, therefore, speed and duration associated with certain speed ranges are used to approximate MSOs. The following describes the MSO model applied for the purpose of this study.

A physiological threshold framework is applied which divides cyclists' power output capacity into five ranges [36], as set out below: (i) Explosiveness (5 s); (ii) Lactic tolerance (30 s); (iii) Maximal aerobic power (∼5 min); (iv) Anaerobic threshold (20–60 min) and (v) Endurance (up to several hours). There are three primary physiological ranges applicable to the durations of the points and scratch races studied, two of which correspond to the ranges of Ref. [36], and one that corresponds to a recovery period. A fourth factor is the reduction in capacity over successive efforts.

The first physiological range is indicated by apparent maximum efforts sustained for 12 s in the points race (51.4 km/h) and 15 s in the scratch race (53.2 km/h). These durations are intermediary to the explosiveness and lactic tolerance ranges of

Table 1
The different ranges of maximal sustainable output (MSO) applied to calculations of Peloton Convergence Ratio (PCR) in this study.

Maximal sustainable output threshold	Points	Scratch
Sprint (lactic tolerance) ("MSO_1")	For speeds between 48 km h and 51.4 km/h of $\leq$30 s, 51.4 km/h is MSO_1.	For speeds between 43.5 km/h and 53.2 km/h of $\leq$30 s, 53.2 km/h is MSO_1.
Recovery MSO ("MSO_R")	72%[a] of MSO_1 of 51.4 km h (747 W[b]) = 537.8 W (45.8 km/h). Four MSO_R periods were counted (Table 2).	72%[a] of MSO_1 53.2 km/h (832 W[b]) = 599 W (47.6 km/h). One MSO_R period was counted of 15 s (9:04–9:18 min) following a 13 s sprint at 48 km/h (Table 2).
Max aerobic power MSO ("MSO_2")	Highest speed sustained for $\geq$30 s but <5 min was 48 km/h. All periods of the race other than for MSO_1 and MSO_R have been counted as MSO_2 using 48 km/h.	Highest speed sustained for $\geq$30 s but <5 min was 43.5 km/h. All periods of the race other than for MSO_1 and MSO_R have been counted as MSO_2 using 43.5 km/h.[c]
Max aerobic power MSO_R	Since speeds were achieved for <5 min, no recovery MSO is observed.	Since speeds were achieved for <5 min, no recovery MSO is observed.
Anaerobic threshold and endurance MSO	Race not sufficiently long for these to be measured.	Race not sufficiently long for these to be measured.

[a] Applying [31–33] 28% reduction in power output during ~15 s recovery periods is used.
[b] Given constant race conditions, speeds may be correlated to power output; power output is calculated using parameters from Ref. [38] and based on rider and bicycle weight of 69 kg.
[c] Includes one event of 19 s, between 8:06 and 8:25 min which is included in this category.

Table 2
Points and scratch races MSO_1 and MSO_R periods.

	Sprint	Period	MSO[1] speed (km/h) [actual speed]	power at actual speed (W) (Pspeed)	MSO_R Recovery period	Recovery Power (W) (Pspeed $*$ 0.72)	MSO speed at Recovery Power (km/h) [actual speed]
Points	1	3:03–3:16	51.4	747	3:17–3:32	537.84	45.8 [39.9]
	2	12:04–12:14	51.4 [48]	614	12:15–12:24	442.1	42.72 [43.5][b]
	3	12:25–12:42	48.32[a] [45]	512	12:43–12:58	368.64	40.04 [39.9]
	4	14:53–15:04	51.4 [48]	614	15:05–15:20	442.1	42.72 [43.5][b]
Scratch	1	8:51–9:03	53.2 [48]	614	9:04–9:18	537.84	45.8 [36.8]
	2	10:27–10:41	53.2 [53.2]	823	None		
	3	10:42–10:45	53.2 [51.4]	747	None		

[a] MSO_{red} (51.4 km/h $*$ 0.94) as a subsequent sprint occurring within 30 s of previous [34].
[b] Actual speed may be higher than MSO since, for all but the front rider, actual power output in drafting positions is reduced according to Peloton Convergence Ratio; although any instance of the front rider exceeding MSO suggests error in the data, here the error is comparatively small and supports the method used in determining a reasonable approximation of MSO.

Table 3
Means for *k*-means clusters sorted for scratch and points races.

Cluster	Scratch race			Points race		
	1	2	3	1	2	3
[a]Density *d*	5.09	5.14	4.27	6.37	5.53	6.19
PCR	0.64	0.52	0.51	0.64	0.495	0.52
Speed	42.15	32.44	32.42	45.68	33.77	37.11
Count	305	186	154	307	316	326

[a] These values are used to determine density $1/d$.

Ref. [36]. For this study, this intermediate maximal effort is referred to as an "MSO_1" event and represents the upper range of maximal efforts achievable by the competitors in this study (Tables 1 and 2). Explosiveness (peak power efforts of up to 5 s) is not identified in the data here.

It is convenient here that all the cyclists' maximum sprint speeds are obtained from 200 m sprint time-trials during the same weekend as the points and scratch races here [37]. This indicates that the top speeds reached in the points (51.4 km/h) and scratch (53.2 km/h) races are indeed close to the cyclists' sprint maxima, and that these top speeds can be applied as benchmark absolute maximal sustainable outputs (MSO_1). The 200 m sprint time average was 14.26 s, indicating that for the races studied here, a reasonable approximation for the maximal sustainable output sprint time is 15 s. In the points race, MSO_1 events were attained during 4 sprint periods, 3 of durations <15 s and one of duration 17 s (Table 2).

The second physiological range applied is a recovery period, referred to as an "MSO_R" event. These correspond to the reported 28% power reduction in capacity between 10 and 20 s of a sprint relative to the first 10 s [31], and similar values [32, 33]. These events are thus calculated as being 72% of an MSO_1 event (Table 2) up to 15 s following an MSO_1 event, as discussed. The third physiological range applied is maximal aerobic power, those efforts of durations in the range 30 s to ~5 min, as noted in Ref. [36]. These are referred to as MSO_2 events (Table 1). The fourth factor involves reductions in output capacity over successive efforts. Where subsequent MSO_1 efforts occurred within <30 s of a previous MSO_1 event, a

reduced MSO_1 value was applied according to the successive fractional outputs indicated in Ref. [32], whereby succeeding sprint efforts are multiplied by 0.94, 0.92, and 0.89 of the initial maximum effort measured. These are referred to as MSO_{red} events. One MSO_{red} was detected in the points race, no MSO_{red} were detected in the scratch race (Table 2).

In applying reduction values, maximal efforts of 6 s are involved in Ref. [34]; here MSO_1 efforts >6 s are applied, meaning that the cyclists in this study likely recovered at a significantly different rate than those in the [34] study. In turn, reductions in successive efforts are likely significantly different than those in the [34] study. However, these reduction values represent reasonable approximations in order to demonstrate the principle of capacity reductions that are expected to occur among competitors in mass-start bicycle races.

3. Results and discussion

3.1. K-means analysis indicates stretched and compact phases

To identify phases and phase boundaries, using NCSS statistical software [39], *k*-means cluster analysis of density (sums of all cyclists' position values, second-to-second) versus Peloton Convergence Ratio produced reasonable phase delineations. Here density is indicated by $1/d$, where d is the sum of the positional-change values, second-to-second (Table 3). Density $1/d$ is therefore lower in the stretched formations, and higher in compact formations.

Different cluster combinations of group density, variations between cyclist position, PCR and speed, and different descriptive statistical parameters such as variance, mean, standard deviation for aggregate positional-change values for each race were evaluated. Comparison of Pearson correlation coefficients for density–PCR versus those for density–speed indicate a higher correlation of density with PCR than with speed (points: 0.602; scratch: 0.412) than density–speed (points: 0.568; scratch: 0.307), providing evidence that the density–PCR is a dominant and appropriate correlate for cluster analysis.

Figs. 3 and 5 show positional-change curves for all riders in the two races for entire race durations. Changes in peloton density $1/d$ are visually apparent, and single-file stretching is indicated in regions where curves run horizontally parallel. Visually there is correspondence between higher PCR and speed and peloton stretching. The data are isolated into statistical groupings according to the density, PCR, and/or speed variables, as shown in Figs. 3 and 5.

Phase distinctions are more readily apparent for the points race data. This may be due to the points race format in which points are awarded every six laps, and the consequent predictable speed increases preceding these points laps. The average speeds for both races were similar (points: 38.7 km/h; scratch 37.1 km/h), but the points race contained 6 periods for which speeds equaled or exceeded 48 km/h, corresponding to points laps (the scratch race contained two such periods). Thus for the scratch race, riders tended to maintain speeds closer to the average for longer periods with lower overall speed, leading to extended mid-range phase activity.

While the points race format allows predictable phase changes preceding points laps there are clearly periods of acceleration occurring on non-points laps, as shown in Figs. 2 and 4. This supports the hypothesized self-organized nature of these events, despite a rigid race format. Cyclists accelerate in this way as a tactic to divide the field before sprint points (or before the finish). The precise timings of such accelerations are not predictable. Indeed, the data indicates acceleration and deceleration periods of unpredictable duration and occurrence, for both the scratch race and the points race.

Thus the points race cluster results indicate a strong distinction between a compact, high density $1/d$ phase, and stretched phase. This phase distinction is somewhat less clear in the clusters shown for the scratch race, while the cluster means indicate some correspondences among low density $1/d$ (stretching), higher PCR and speeds. Since reasonable correlation between stretching and high PCR (and speed) occurs in two types of racing conditions – one in the points race where high speeds are predicted to precede points laps, and the second in the scratch race, where periods of high speed occur unpredictably – there is sufficient evidence to conclude that the stretched phase is a separate phase from a higher density $1/d$ – compact – phase.

3.2. Dividing the compact phase into a synchronized phase and convective or disordered phase

The cluster analysis is less clear in distinguishing among the constituent sub-phases of the compact condition. However, lagged cross-correlation analysis of variance and density indicate correlations among lagged versions of the variables that were not revealed previously by the *k*-means cluster analysis. Here variance is the variance in the usual statistical sense, of riders' position values, with respect to their mean (on a second-to-second basis, as usual). The lagged correlations are shown in Fig. 6. A significant positive correlation lag appears for both races, indicating that density $1/d$ may remain stable for periods while cyclists' rates of positional-change vary. This is evident in the periods of lateral synchrony indicated by the yellow arrow in Figs. 4 and 5; also in Fig. 5, where the period following the yellow arrow region exhibits an obvious increase in frequency of positional-change but sustains approximately the same density $1/d$, as indicated by the cluster mean density. The relatively low Pearson correlation between variance–PCR (points: 0.153; scratch 0.104) and variance–speed (points: 0.134; scratch: 0.118) may also explain why no additional resolution is added to the cluster analysis by including variance and density together, while the comparatively high cross-correlation for density–PCR and density–speed indicates a distinction between a compact synchronized phase, and a compact high frequency positional-change phase. Compact, high frequency positional-change phases may exhibit convective motion, or disordered, non-convective motion, although these distinctions have not been quantified here.

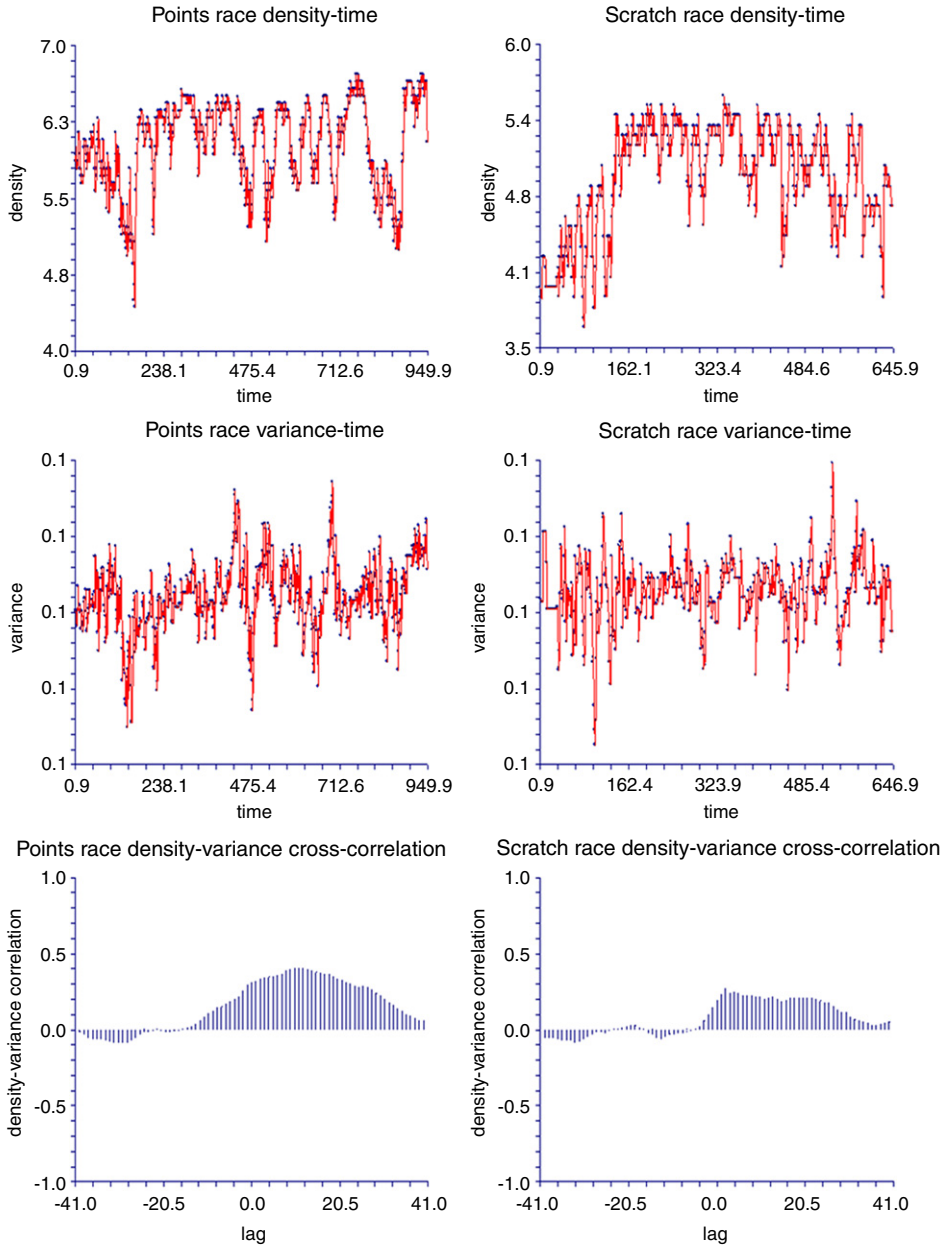

Fig. 6. Lagged correlations between variance and density in the points and scratch races. Points race shown in left column; scratch race in right column. Peak correlations: 0.409 for points race at lag point 14; 0.215 for scratch race at lag point 17.

3.3. Basic mechanics of a peloton phase transition

It may assist understanding of peloton dynamics to illustrate the basic mechanics of peloton phase transitions. Fig. 7(a) shows a compact disordered (or convective) phase. In this phase, riders pass on perimeters due to high internal density $1/d$, while riders in the central region move effectively backward (shown by short straight arrow). The curved arrows show the directions of cyclists at the perimeters, and the long straight arrow shows the direction of the peloton.

In Fig. 7(b), as speeds increase such that cyclists approach maximal sustainable output, the direction of collective motion shifts as cyclists seek optimal drafting positions. At the transition between a compact and a stretched phase, speeds are sufficiently high such that cyclists can no longer pass around peloton perimeters or sustain a non-drafting position (or if they can, it is energetically very costly to do so) and a phase transition occurs. In Fig. 7(c), the phase transition is complete, resulting in a stretched formation. In Fig. 7(b) and (c), the green arrows depict gap formation.

In Fig. 7(b) cyclist B is at PCR $>$ 1 relative to cyclist A. If riders behind B are at PCR $<$ 1 relative to A, they may maintain contact with the peloton by laterally shifting towards drafting positions (or passing, if it is not too energetically costly). In

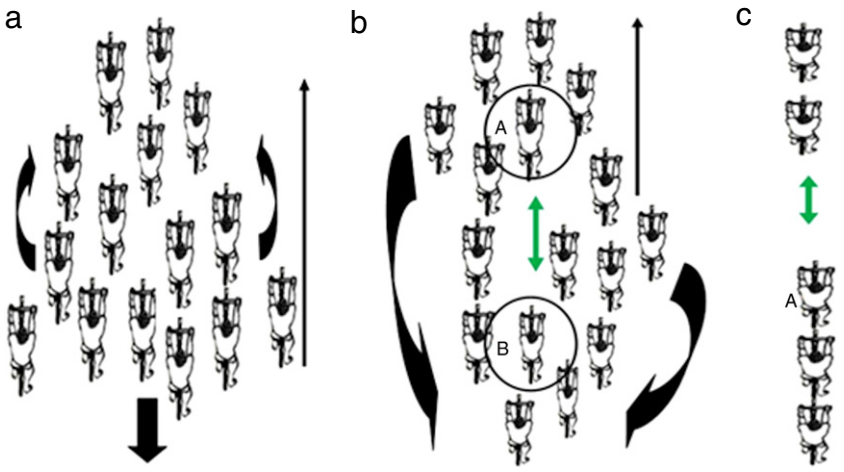

Fig. 7. Illustrating a peloton phase transition: (a) curved arrows indicate direction of cyclists' motion as riders pass on peripheries; short straight arrow indicates effective direction of motion of cyclists moving backward relative to those passing on peripheries; long arrow indicates actual direction of peloton motion; (b) curved arrows indicate effective direction of motion for riders at PCR $>$ 1 relative others at the head of the group; green arrow indicates gap formation between riders at PCR $>$ 1 relative to each other; (c) stretched formation in which it is too energetically costly for riders to pass on peripheries; green arrow indicates gap formation between rider A at PCR $>$ 1 to the rider ahead. (For interpretation of the references to color in this figure legend, the reader is referred to the web version of this article.)

Fig. 7(c), however, it will be more difficult for following riders to pass A since, even if they are at PCR $<$ 1 while drafting, some must pass in a non-drafting position which may result in reaching PCR $>$ 1 in doing so. Peloton divisions may occur in both Fig. 7(b) and (c), but are more likely to occur in Fig. 7(c). As a peloton slows its pace, a phase transition will occur in the opposite direction by general convective motion as riders pass others on peloton peripheries.

3.4. Phase symmetry

The illustration in Fig. 7 also indicates phase symmetry: the compact convective process occurs in both directions: cyclists' deliberate forward movement to achieve front positions during an acceleration period generates convection or a disordered state, but the convective motion may also occur during collective deceleration as fresher riders pass fatiguing ones. Similarly, a backward convection may occur during a transition to a stretched state during acceleration.

In certain conditions and in view of varying rates of fatigue and recovery, cyclists within a comparatively broad range of physiological capacities and maximal sustainable outputs and temporary PCR may be moving backward and forward simultaneously within a peloton. These reasons for constant motion within the peloton are in addition to constant smaller adjustments at lower scales, including braking and accelerating to avoid collisions. During periods of collective fatigue, cyclists decelerate and phases appear to be sustained at slower speeds, until cyclists recover and then resume phases through an acceleration period.

The data indicates phase symmetry between acceleration and deceleration periods, in that phases retain PCR and density $1/d$ characteristics but during opposite directions in speed. Thus a compact phase, characterized by low positional-change and high density $1/d$, appears to have a counterpart refractory phase at higher speed but occurs after a short-term period of high power output when cyclists are resting and regenerating energetic resources. Further work is required to quantify this. Also, further analysis is required to clearly demonstrate empirically the presence of convective motion. More precise maximal sustainable outputs and timing data may reveal acceleration/deceleration phase symmetry more accurately.

3.5. Peloton divisions

The mechanism for the division of a peloton into sub-pelotons provides insight into the genesis of group divisions within other biological systems, and how such groups may diverge and ultimately propagate independently.

Peloton phases may be unstable at high aggregate power outputs, particularly in the stretched phase. Separation between riders occurs where PCR $>$ 1, but the relative size of the peloton allows riders at PCR $>$ 1 to stay within the group accordingly:

$$T_{\text{gap}} = \frac{D_{\text{last}}}{(S_p - S_{\text{pcr}} > 1)} \tag{3}$$

where T_{gap} is the time required for a given rider to reach the back of the pack, as shown in Fig. 8; D_{last} is the distance between that rider's current position and the last rider in the pack; S_p is the current average speed of the peloton as determined by the front rider; $S_{\text{pcr}>1}$ is the speed of the given rider at PCR $>$ 1 (whose speed must be slower than the pack).

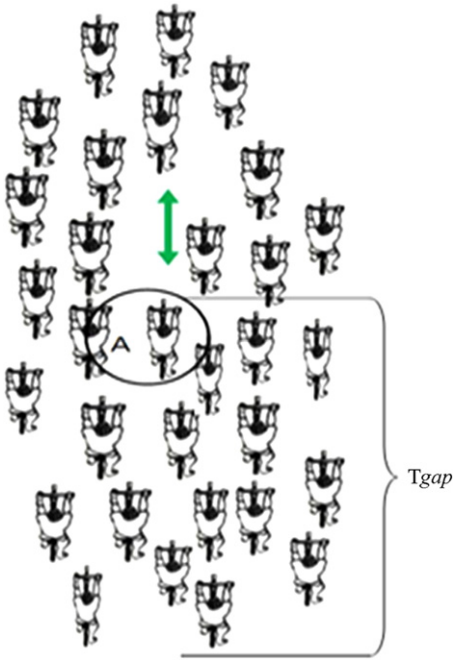

Fig. 8. Illustrating a peloton division: rider A is PCR $>$ 1 relative to the rider ahead, and decelerates relative to the group. The green arrow indicates increasing separation between rider A and the rider ahead. T_{gap} is the distance between rider A and the rear-most drafting position in the peloton; T_{gap} increases as the peloton lengthens. Because a peloton consists of many riders (e.g. the Tour de France consists of ∼200 riders), even when riders exceed their maximal sustainable outputs, all is not lost if the pace slows before they are separated from the group.

If a rider is at Peloton Convergence Ratio $>$ 1 for $t > T_{\text{gap}}$, he or she will separate from the group; more than one rider at $t > T_{\text{gap}}$, and the peloton divides in groups. If a group elongates, as in Fig. 7(c), T_{gap} is increased. Hence, in addition to or complementary to other causes of swarming behavior [40] among collectives in which energy savings mechanisms exist, (3) models how group divisions occur and suggests why larger groups may confer an evolutionary advantage and a wider range of physiological heterogeneity than smaller groups.

This illustration models elements of cyclists' continually changing positions within a peloton, and explains why it is advantageous to stay near the front of the peloton, why a larger pack is advantageous for all riders, and why weaker riders may maintain pace with a peloton for an entire race.

4. Summary and outlook

By deriving positional-changes (2) from video data from two mass-start track cycling races, important parameters were obtained that illuminate the dynamic interrelations among cyclists' positions over time. Despite the coarse-grained timing available for the speed data and simplifying assumptions used in the evaluation of parameters maximal sustainable output (MSO) and drafting parameter D, analysis of the data allowed evidence to be obtained of two primary phases: a stretched, low density $1/d$ phase, and high density $1/d$ phase. The stretched phase occurs in the highest range of Peloton Convergence Ratio (PCR) and speed, and is indicated by low frequencies and magnitudes of positional-change.

The high density $1/d$ phase may be divided into two further phases, one which exhibits lateral synchrony and occurs for intermediate PCR values, and another that is characterized by a similar density $1/d$ but occurs at higher frequencies and magnitudes of positional-change. The evidence for a convective phase (in the sense of cyclists passing on periphery) has not yet been demonstrated from the data. However, the frequent re-ordering of cyclists during this phase (as indicated by high frequency variations in the positional-change variable) may include convective motion. Refined methods to identify specific positional-change trajectories are required to empirically reveal convective motion. Further, given the relatively small peloton sizes observed here, it is not clear whether sufficiently many riders were present in order for clear convective motion to develop.

In summary, the evidence supports the following phase descriptions: (i) Relaxed ("compact"): high density $1/d$ low frequency–magnitude positional-change; intermediate values of PCR $<$ 1. Cyclists proceed at comparatively low power outputs; lateral synchronization is present; (ii) Disordered ("compact"): high density $1/d$, high frequency–magnitude positional-change; low to mid range PCR $<$ 1; (iii) Stretched: low density $1/d$, low frequency–magnitude positional-change; high PCR $<$ 1; single-file synchronization is present.

Examples of the high density $1/d$ phases can be seen in the original video of the scratch race available at http://www.youtube.com/watch?v=an2cLWSq2vM at 1:45–2:10 (phase I) and 7:20–7:35 (phase II). Examples of the low density $1/d$ (phase III) can be seen in the same video at 4:55–5:10 and 7:50–8:10.

In addition to increasing our understanding of peloton dynamics specifically, the study of peloton phase dynamics provides understanding of general processes underlying separation of individuals or subgroups from larger collectives, in the presence of energy savings mechanisms. As such, an understanding of peloton dynamics may well shed light on the role of energy savings mechanisms within evolutionary processes. For example, further study of maximal aerobic capacity and range of heterogeneity and energy savings within different kinds of biological collectives, such as in Ref. [41] for fish schooling dynamics, may provide further insight into the evolutionary implications of the phase dynamics and collective behavior of pelotons. Similar studies may be undertaken for a variety of biological systems.

References

[1] C. Castellano, S. Fortunato, V. Loreto, Statistical physics of social dynamics, Rev. Modern Phys. 81 (2009) 591.
[2] G. Szabo, G. Fath, Evolutionary games on graphs, Phys. Rep. 446 (2007) 97.
[3] M. Perc, A. Szolnoki, Coevolutionary games—a mini review, Biosystems 99 (2010) 109.
[4] M. Perc, et al., Evolutionary dynamics of group interactions on structured populations: a review, J. R. Soc. Interface 10 (2013) 20120997.
[5] H.E. Stanley, Introduction to Phase Transitions and Critical Phenomena, Clarendon Press, Oxford, 1971.
[6] E. Ising, Beitrag zur theorie des ferromagnetismus, Z. Phys. 31 (1925) 253.
[7] V. Tamás, Fractal Growth Phenomena, World Scientific, Singapore, 1989.
[8] A.L. Barabasi, H.E. Stanley, Fractal Concepts in Surface Growth, Cambridge University Press, Cambridge, 1995.
[9] R.N. Mantegna, H.E. Stanley, Introduction to Econophysics: Correlations and Complexity in Finance, Cambridge University Press, Cambridge, 2000.
[10] I. Couzin, et al., Effective leadership and decision-making in animal groups on the move, Nature 433 (2005) 513.
[11] H. Trenchard, Peloton phase oscillations, Chaos Solitons Fractals 56 (2013) 194.
[12] S. Padilla, I. Mujika, J. Orbananos, J. Santisteban, F. Angulo, J.J. Goiriena, Exercise intensity and load during mass-start stage races in professional road-cycling, Med. Sci. Sports Exerc. (2000) 796.
[13] E. Martins Ratamero, MOPED: an agent-based model for peloton dynamics in competitive cycling, in: International Congress on Sports Science Research and Technology Support, 2013, Vilamoura, icSPORTS, 2013.
[14] J. Zhang, W. Mehner, E. Andresen, S. Holl, M. Boltes, A. Schadschneider, A. Seyfried, Comparative analysis of pedestrian, bicycle and car traffic moving in circuits, Proc. Soc. Behav. Sci. 104 (2013) 1130.
[15] S. Zhang, G. Ren, R. Yang, Simulation model of speed–density characteristics for mixed bicycle flow—comparison between cellular automata model and gas dynamics model, Physica A 392 (20) (2013) 5110.
[16] A. King, A. Wilson, S. Wilshin, J. Lowe, H. Haddadi, S. Halles, J. Morton, Selfish-herd behavior of sheep under threat, Curr. Biol. 22 (14) (2012) R561.
[17] A. De Vos, M. O'Rain, Sharks shape the geometry of a selfish seal herd: experimental evidence from seal decoys, Biol. Lett. 6 (2010) 48.
[18] S. Viscido, D. Wethey, Quantitative analysis of fiddler crab flock movement: evidence for 'selfish herd' behaviour, Anim. Behav. 63 (4) (2002) 735.
[19] S. McCole, K. Claney, J. Conte, R. Anderson, J. Hagberg, Energy expenditure during bicycling, J. Appl. Physiol. 68 (2) (1990) 748.
[20] T. Olds, The mathematics of breaking away and chasing in cycling, Eur. J. Appl. Physiol. 77 (1998) 492.
[21] C. Kyle, Reduction of wind resistance and power output of racing cyclists and runners travelling in groups, Ergonomics 22 (1979) 387.
[22] T. Compton, 2001. http://www.analyticcycling.com/ForcesPower_Page.html.
[23] B. Blocken, T. Defraeye, E. Koninckx, J. Careliet, P. Hespel, CFD simulations of the aerodynamic drag of two drafting cyclists, Comput. Fluids 71 (2013) 435.
[24] M. Black, J. Durant, A. Jones, A. Vanhatalo, Critical power derived from a 3-min all-out test predicts 16.1-km road time-trial performance, Eur. J. Sport Sci. 1 (2013).
[25] O. Faude, W. Kinderman, T. Meyer, Lactate threshold concepts—how valid are they? Sports Med. 39 (6) (2009) 469.
[26] W. Bertucci, R. Taiar, Y. Toshev, T. Letellier, Comparison of biomechanical criteria in cycling maximal effort test, Int. J. Sports Sci. Eng. 2 (1) (2008) 36.
[27] G. Rodas, J. Ventura, J. Cadefu, R. Cusso, J. Parra, A short training programme for the rapid improvement of both aerobic and anaerobic metabolism, Eur. J. Appl. Physiol. 82 (2000) 480.
[28] G. Bogdanis, M. Nevill, Boobis, H. Lakomy, A. Nevill, Recovery of power output and muscle metabolites following 30 s of maximal sprint cycling in man, J. Physiol. 482 (2) (1995) 467–480.
[29] H. Bergstrom, T. Housh, J. Zuniga, C. Camic, D. Traylor, R. Schmidt, G. Johnson, Estimated times to exhaustion and power outputs at the gas exchange threshold, physical working capacity at the rating of perceived exertion threshold, and respiratory compensation point, Appl. Physiol. Nutr. Metab. 37 (2012) 872.
[30] D. Bishop, Fatigue during intermittent sprint exercise, Proc. Aust. Physiol. Soc. 43 (2012) 9.
[31] G. Bogdanis, M. Nevill, H. Lakomy, L. Boobis, Power output and muscle metabolism during and following recovery from 10 and 20 s of maximal sprint exercise in humans, Acta Physiol. Scand. 163 (3) (1998) 261.
[32] M. Glaister, M. Stone, A. Stewart, M. Hughes, G. Moir, The influence of endurance training on multiple sprint cycle performance, J. Strength Cond. Res. 21 (2) (2007) 606.
[33] M. Glaister, M. Stone, A. Stewart, M. Hughes, G. Moir, The influence of recovery duration on multiple sprint cycling performance, J. Strength Cond. Res. 19 (4) (2005) 831.
[34] A. Mendez-Villanueva, J. Edge, R. Suriano, P. Hamer, D. Bishop, The recovery of repeated-sprint exercise is associated with PCr resynthesis, while muscle pH and EMG amplitude remain depressed, PLoS One 7 (12) (2012) e51977.
[35] R. Lukes, M. Carre, S. Haake, Track cycling: an analytical model, Eng. Sport 6 (2006) 115.
[36] J. Pinot, F. Grappe, The 'power profile' for determining the physical capacities of a cyclist, Comput. Meth. Biomech Eng. 13 (S1) (2010) 103.
[37] http://www.gvva.bc.ca/provincials/.
[38] www.bikecalculator.com.
[39] J. Hintze, NCSS 2007. NCSS, LLC. Kaysville, Utah, USA, 2007. www.ncss.com.
[40] T. Vicsek, A. Zafeiris, Collective motion, Phys. Rep. 517 (3–4) (2012) 71.
[41] S. Killen, S. Marras, J. Steffensen, D. McKenzie, Aerobic capacity influences the spatial position of individuals within fish schools, Proc. R. Soc. B 279 (2012) 357.